A Level Set Method by Characteristic-based Finite Volume Formulation for Rectangular Grid

Sutthisak Phongthanapanich[1]

บทคัดย่อ

วิธีเซตของระดับโดยอาศัยรูปแบบของไฟไนต์วอลุ่มคุณลักษณะถูกนำเสนอ วิธีดังกล่าวสามารถแก้ปัญหาการเคลื่อนตัวของผิวรอยต่อพร้อมกับเซตของระดับศูนย์ แนวคิดของเทคนิคคุณลักษณะถูกนำมาใช้ในการสร้างสมการเซตของระดับในสองมิติ สูตรไฟไนต์วอลุ่มแบบชัดแจ้งถูกนำมาใช้ในการสร้างสมการสำหรับตาข่ายรูปแบบใดๆ บทความนี้มุ่งเน้นการจำลองเชิงตัวเลขของการพาผิวรอยต่อของปัญหาพลศาสตร์ของไหลของพื้นผิวอิสระ กรณีตัวอย่างหลากหลายได้ถูกใช้ในการประเมินสมรรถนะของวิธีที่ถูกนำเสนอทั้งในกรณีของการไหลแบบคงตัวและไม่คงตัว ผลลัพธ์ที่ได้ถูกนำมาเปรียบเทียบกับผลลัพธ์แม่นตรงหรือผลลัพธ์ที่ปรากฏในเอกสารวิจัยอื่น

คำสำคัญ: สมการเซตของระดับแบบคุณลักษณะ ระเบียบวิธีไฟไนต์วอลุ่ม วิธีชัดแจ้ง

Abstract

A level set method based on the characteristic finite volume formulation is presented. The method solves the evolving interface problems with zero level set along their interfaces. The idea of the characteristic-based technique is implemented to derive a level set equation in two dimensions. An explicit finite volume formulation is employed to discretize the equations applicable for arbitrary grids. The paper focuses on numerical simulation of the interface advection equation for free-surface fluid dynamics problems where the naive finite element method yields unsatisfactory solutions. Several test cases are presented to evaluate the performance of the proposed method on both steady and transient flow fields. The derived results are compared with the exact solutions or those in the literatures.

Keywords: Characteristic Level Set Equation, Finite Volume Method, Explicit Scheme

1. Introduction

Interface evolution problems consist of capturing or tracking the motion of their interfaces as they evolve. Several techniques have been developed to predict the behavior, such as by using Marker-and-Cell (MAC) [1], Volume-of-Fluid (VOF) [2] and level set methods [3]. The level set methods have gained popularity mainly because of its simplicity in formulation and implementation. Applications of the level set methods for moving boundaries and interfaces problems exist in many fields such as the crystal and crack growth, bubbles and droplets deformation,

[1] Associate Professor, Department of Mechanical Engineering Technology, College of Industrial Technology, King Mongkut's University of Technology North Bangkok, Tel. 0-2587-3921, E-mail: sutthisakp@kmutnb.ac.th

Received 10 May 2011; Accepted 22 November 2011

multiphase flows, multifluid flows, front propagations and fluid-structural interactions [3]-[7]. Numerical simulation of the interface motion problems using the level set principle is determined by advecting a relatively smooth field, ϕ, whose zero level set is the interface. Flows near the interfaces often have strong vortical components because of the related sharp gradients in the fluid flow properties. To predict the flow phenomena accurately, the interface needs to be tracked precisely in both time and space. Many numerical techniques with high-order solution accuracy have been introduced to discretize the level set equation such as the finite difference, finite element and finite volume methods. The objective of this work is to develop an explicit finite volume method for solving the characteristic level set equation in two-dimensional domain. In this paper, the concept of characteristic-based scheme [8], for approximating the Lagrangian derivatives in time, is used to derive the characteristic level set equation. An explicit finite volume method is applied to the characteristic level set equation to develop the discretized equations for the spatial domain. Due to the virtue of the characteristic level set equation, the proposed method provides the second-order accurate solutions in time without using the multi-stages Runge-Kutta time stepping scheme such as those in the second-order TVD-RK or the fourth-order RK schemes. Only one turn of computation is needed to obtain the solution at time t^{n+1}. Hence, the method requires less physical memory and CPU time. Robustness and efficiency of the proposed method are examined by analyzing two-dimensional examples. Results are compared with the known analytical solutions and/or those reported by other researchers. The presentation of the paper starts from explaining the theoretical formulation and corresponding characteristic-based scheme in Section 2. The conventional finite volume discretization of the characteristic level set equation is further presented in this section. Lastly, performance of the proposed method is examined and evaluated in Section 3 by using two examples. These examples are: (1) the circulation of an expanding and shrinking circle, and (2) the time-reversed vortex test.

2. Derivation of Characteristic Level Set Equation

The level set methods have been used widely to determine evolution for interface problems because of its simplicity and ability to capture topological changes such as shrinking, merging, and splitting easily without applying any special treatment technique. For a two-dimensional domain, the advection-diffusion form for the level set function is,

$$\frac{\partial \phi}{\partial t} + \boldsymbol{v} \cdot \nabla \phi = 0 \tag{1}$$

where $\phi = \phi(\boldsymbol{x}, t)$ defines the implicit interface by its zero level set, and is chosen to be positive outside, $\Omega\,(\Omega^{+})$, negative inside $\Omega\,(\Omega^{-})$, and zero on interface $(\partial\Omega_I)$, and $t \in (0, T)$ for $T < \infty$. The velocity field $\boldsymbol{v} = \boldsymbol{v}(\boldsymbol{x}, \nabla\phi(\boldsymbol{x}, t), t)$ can be defined in several ways depending on applications [3]. For an example, the externally generated velocity field (advection) is $\boldsymbol{u}(\boldsymbol{x}, t)$, the velocity field for constant motion in the normaldirection is $a\nabla\phi/|\nabla\phi|$, and the curvature is $\kappa = \nabla \cdot (\nabla\phi/|\nabla\phi|)$. The initial condition is defined for $\boldsymbol{x} \in \Omega$ with $\Omega \subset R^2$ and by $\Omega = \Omega^{+} \cup \Omega^{-} \cup \partial\Omega_I$ by $\phi(\boldsymbol{x}, 0) = \phi_0(\boldsymbol{x})$.

By following the procedure described in Refs. [8], Eq. (1) is semi-discretized along the characteristic line so that it can be written in the form

$$\frac{1}{\Delta t}\left(\phi^{n+1}\Big|_{x} - \phi^{n}\Big|_{x-\Delta x}\right) = 0 \tag{2}$$

where $\phi = \phi(\boldsymbol{x}', t)$ and $\boldsymbol{x}'$ is the path of the characteristic wave. The incremental time period Δt is from n to n+1, and the incremental distance $\Delta \boldsymbol{x}$ is from $\boldsymbol{x} - \Delta \boldsymbol{x}$ to $\boldsymbol{x}$. The local Taylor series expansion in space is applied to the second term on the left-hand side of the equation. The incremental distance $\Delta \boldsymbol{x}$ along the characteristic path is then approximated by $\Delta \boldsymbol{x} = \boldsymbol{V}^{n+1/2} \Delta t$, where $\boldsymbol{V}^{n+1/2}$ where is the average velocity along the characteristic at time t=n+1/2 [8]. Equation (2) can then be written in the fully explicit form

$$\frac{1}{\Delta t}(\phi^{n+1} - \phi^n) = \left[-\boldsymbol{V} \cdot \nabla \phi + \frac{\Delta t}{2} (\nabla \phi \boldsymbol{V} \cdot \nabla \boldsymbol{V} + \boldsymbol{V} \boldsymbol{V} \cdot \nabla^2 \phi) \right]^n \quad (3)$$

By utilizing some vector identity, the semi-discrete form of the characteristic level set equation becomes

$$\frac{1}{\Delta t}(\phi^{n+1} - \phi^n) = \left[-\boldsymbol{V} \cdot \nabla \phi + \frac{\Delta t}{2} \boldsymbol{V} \cdot \nabla \boldsymbol{V} \cdot \nabla \phi \right]^n \quad (4)$$

Finally, Eq. (4) can be written preferably in the conservation form for applying the finite volume method as

$$\begin{aligned} \phi^{n+1} - \phi^n = & -\Delta t \left[\nabla \cdot (\boldsymbol{V} \phi) + \phi \nabla \cdot \boldsymbol{V} \right]^n \\ & + \frac{(\Delta t)^2}{2} \left[\nabla \cdot (\boldsymbol{V} \nabla \phi \cdot \boldsymbol{V}) - \boldsymbol{V} \cdot \nabla \phi \nabla \cdot \boldsymbol{V} \right]^n \end{aligned} \quad (5)$$

The computational domain is first discretized into a collection of non-overlapping convex polygon control volumes $\Omega_i \in \Omega, i = 1, ..., N$, that completely cover the domain such that $\Omega = \cup_{i=1}^{N} \Omega_i$, $\Omega_i \neq 0$, and $\Omega_i \cap \Omega_j = 0$ if $i \neq j$. Equation (5) is integrated over the control volume Ω_i to obtain

$$\begin{aligned} \int_{\Omega_i} \phi^{n+1} - \phi^n d\boldsymbol{x} = & -\Delta t \int_{\Omega_i} \left[\nabla \cdot (\boldsymbol{V} \phi) + \phi \nabla \cdot \boldsymbol{V} \right]^n d\boldsymbol{x} \\ & + \frac{(\Delta t)^2}{2} \int_{\Omega_i} \left[\nabla \cdot (\boldsymbol{V} \nabla \phi \cdot \boldsymbol{V}) - \boldsymbol{V} \cdot \nabla \phi \nabla \cdot \boldsymbol{V} \right]^n d\boldsymbol{x} \end{aligned} \quad (6)$$

The divergence theorem is applied to some spatial terms on the right-hand side to yield

$$\begin{aligned} \int_{\Omega_i} \phi^{n+1} d\boldsymbol{x} = & \int_{\Omega_i} \phi^n d\boldsymbol{x} \\ & - \Delta t \int_{\partial \Omega_i} \hat{\boldsymbol{n}}_i \cdot \left[\boldsymbol{V} \phi - \frac{\Delta t}{2} \boldsymbol{V} \nabla \phi \cdot \boldsymbol{V} \right]^n d\sigma \\ & + \Delta t \int_{\Omega_i} \left[\phi \nabla \cdot \boldsymbol{V} - \frac{\Delta t}{2} \boldsymbol{V} \cdot \nabla \phi \nabla \cdot \boldsymbol{V} \right]^n d\boldsymbol{x} \end{aligned} \quad (7)$$

where $\hat{\boldsymbol{n}}_i$ is the unit outward normal vector of $\partial \Omega_i$. The approximation to the cell average of ϕ over Ω_i at time and is represented by [9]

$$\phi_i^n = \frac{1}{|\Omega_i|} \int_{\Omega_i} \phi^n d\boldsymbol{x} \quad (8a)$$

$$\phi_i^{n+1} = \frac{1}{|\Omega_i|} \int_{\Omega_i} \phi^{n+1} d\boldsymbol{x} \quad (8b)$$

where $|\Omega_i|$ is the measure of Ω_i. For any control volume, the flux integral over $\partial \Omega_i$ that appears on the right-hand side of Eq. (7) may be approximate by the summation of fluxes passing through all adjacent cell faces. Hence, by applying the midpoint quadrature integration rule to the second term on the right-hand side of Eq. (7) [8],[9], the flux integral over $\partial \Omega_i$ is

$$\int_{\partial \Omega_i} \hat{\boldsymbol{n}}_i \cdot \left[\boldsymbol{V} \phi \right]^n d\sigma \approx \sum_{j=1}^{4} \left| \Gamma_{ij} \right| \hat{\boldsymbol{n}}_{ij} \cdot \boldsymbol{V}_{ij}^n \phi_{ij}^n \quad (9)$$

$$\begin{aligned} & \Delta t \int_{\partial \Omega_i} \hat{\boldsymbol{n}}_i \cdot \left[\frac{\Delta t}{2} \boldsymbol{V} \nabla \phi \cdot \boldsymbol{V} \right]^n d\sigma \approx \\ & \frac{(\Delta t)^2}{2} \boldsymbol{V}_i^n \cdot \nabla \phi_i^n \sum_{j=1}^{4} \left| \Gamma_{ij} \right| \hat{\boldsymbol{n}}_{ij} \cdot \boldsymbol{V}_{ij}^n \end{aligned} \quad (10)$$

The terms that appear in the third integration term on the right-hand side of Eq. (7) are approximated as source terms by

$$\int_{\Omega_i} \left[\phi \nabla \cdot \boldsymbol{V} \right]^n d\boldsymbol{x} \approx \phi_i^n \sum_{j=1}^{4} \left| \Gamma_{ij} \right| \hat{\boldsymbol{n}}_{ij} \cdot \boldsymbol{V}_{ij}^n \quad (11)$$

$$\begin{aligned} & \int_{\Omega_i} \left[\frac{\Delta t}{2} \boldsymbol{V} \cdot \nabla \phi \nabla \cdot \boldsymbol{V} \right]^n d\boldsymbol{x} \approx \\ & \frac{\Delta t}{2} \boldsymbol{V}_i^n \cdot \nabla \phi_i^n \sum_{j=1}^{4} \left| \Gamma_{ij} \right| \hat{\boldsymbol{n}}_{ij} \cdot \boldsymbol{V}_{ij}^n \end{aligned} \quad (12)$$

where Γ_{ij} is the segment of boundary $\partial\Omega_i$ between two adjacent control volumes Ω_i and Ω_j, which are defined by and $\partial\Omega_i = \cup_{j=1}^{NF}\Gamma_{ij}$ and $\Gamma_{ij} = \partial\Omega_i \cap \partial\Omega_j$.

By substituting Eqs. (8)-(12) into Eq. (7), a fully explicit formulation for solving a characteristic level set equation (Eq. (5)) is obtained as

$$\phi_i^{n+1} = \phi_i^n - \frac{\Delta t}{|\Omega_i|}\sum_{j=1}^{4}|\Gamma_{ij}|\hat{\boldsymbol{n}}_{ij}\cdot\boldsymbol{V}_{ij}^n\left[\phi_{ij}^n - \frac{\Delta t}{2}\left(\boldsymbol{V}_i^n\cdot\nabla\phi_i^n\right)\right] + \frac{\Delta t}{|\Omega_i|}\left(\phi_i^n - \frac{\Delta t}{2}\left(\boldsymbol{V}_i^n\cdot\nabla\phi_i^n\right)\right)\sum_{j=1}^{4}|\Gamma_{ij}|\hat{\boldsymbol{n}}_{ij}\cdot\boldsymbol{V}_{ij}^n \quad (13)$$

The level set function for the cell face at time step t^n, ϕ_{ij}^n, is approximated by applying the Taylor series expansion in space such that

$$\phi_{ij}^n = \phi_i^n + (\boldsymbol{x}_{ij} - \boldsymbol{x}_i)\cdot\nabla\phi_i^n \quad (14)$$

Where x_i and x_{ij} are the cell centroid and the face centroid locations, respectively, as shown by an example of the quadrilateral grids in Fig. 1. For opposite direction of velocity, the values of ϕ_{ij}^n may be computed from Eq. (14) but by using the values from the neighboring control volumes according to the upwinding direction, such that $\phi_{ij}^n = \phi_j^n + (\boldsymbol{x}_{ij} - \boldsymbol{x}_j)\cdot\nabla\phi_j^n$.

3. Numerical Examples

To evaluate the robustness and accuracy of the proposed second-order characteristic level set approach, two examples are examined. These examples are: (1) the circulation of an expanding and shrinking circle, and (2) the time-reversed vortex test.

3.1 Circulation of An Expanding and Shrinking Circle

The first tested case is a circulation of an expanding and shrinking circle in a square domain of $\Omega = (-1,-1)\times(1,1)$. This example also has an analytical solution derived from the Huygens' principal so that the computed solution can be compared. Initially, the circle with radius of 0.25 is centered at (-0.4,0) and is rotated with a non divergence-free velocity field (advection velocity and interface normal velocity). At time $t = [0,1]$ the velocity field is given by

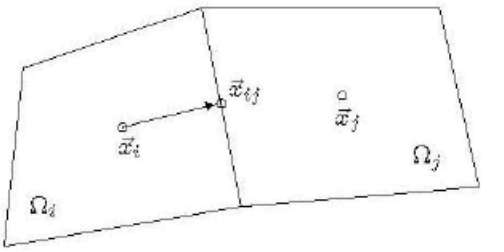

Figure 1 Two control volumes and adjacent cell face.

$$\boldsymbol{V}(\boldsymbol{x}) = (2\pi y, -2\pi x) + 0.1\frac{\nabla\phi}{|\nabla\phi|} \quad (15)$$

The circle is expanding and rotating in the clockwise direction. At a later time of $t = [1,2]$ the velocity field is reversed such that

$$\boldsymbol{V}(\boldsymbol{x}) = (-2\pi y, 2\pi x) - 0.1\frac{\nabla\phi}{|\nabla\phi|} \quad (16)$$

The circle is then shrinking and rotating in the counter-clockwise direction. The exact solution at the final time is the same as the initial condition. To assess the performance and order of convergence of the scheme, the simulations are performed on the four uniform square grids S1 to S4 consisting of 32×32 $(\Delta x = \Delta y = 1/32)$, 64×64, 128×128, and 256×256, respectively. The zero level contour plots of the exact and numerical solutions obtained from grids S1 to S4 at the four different times of 0.5, 1.0, 1.5, and 2.0 are presented in Figs. 2(a)-(d), respectively. These figures show that at the final time $t = 2$, the difference of the interface position between the exact and

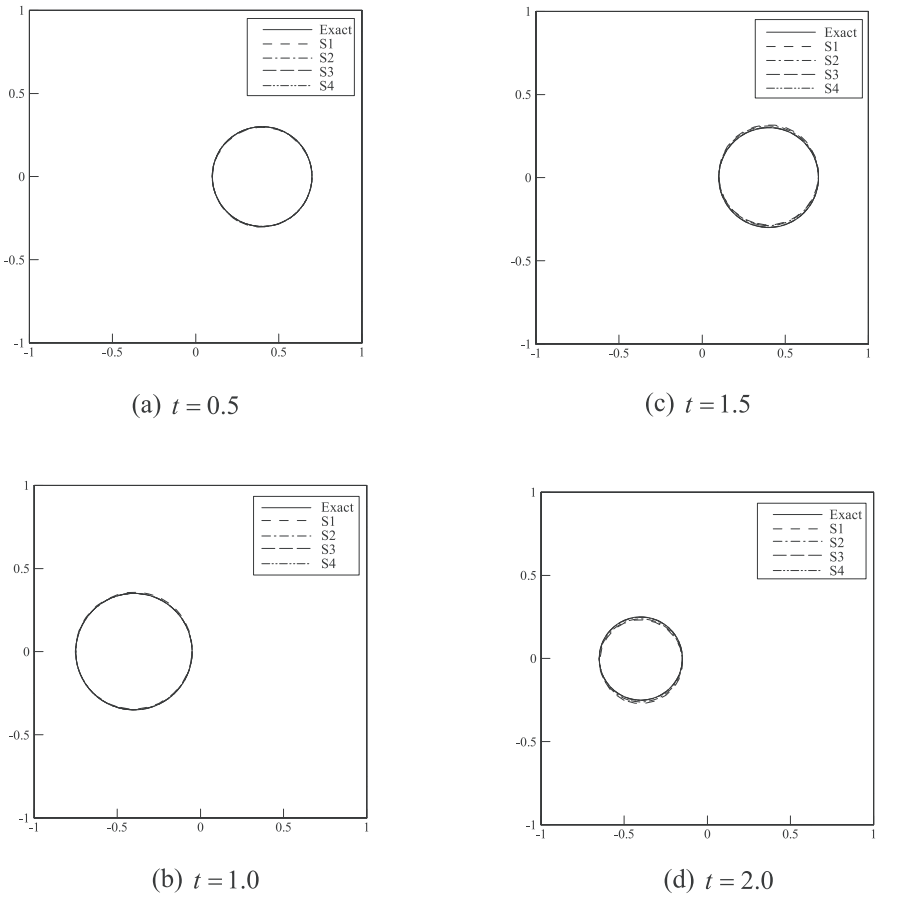

Figure 2 Comparison of exact and numerical solutions of problem 3.1.

numerical solutions is very small for grids S3 and S4. These solutions highlight the ability of the proposed method that can provide nearly circular interface simulation even though some grid sizes are relatively coarsened such as grids S1 or S2

In the application of level set method for solving the incompressible two-phase flow problems, the calculation of the normal vectors is important. The accuracy of the predicted normal vectors is measured by plotting the level set contours and normal vectors obtained from grids S1 and S2 in Figs. 3(a)-(b), respectively. The level set contours are distorted near the upper-left boundaries and the normal vectors are not perpendicular to the level set contours for grid S1. The solution accuracy for both the level set contours and normal vectors are improved for the finer grid S2. Figure 4 shows the distribution of level set function at time obtainedfrom the S grids (grid S4) for which the signed distance function is preserved during the simulation.

The $L_{1,1}$ -norm of the numerical error is used to measure the difference of the numerical interface position from the exact solution. The error is defined by [10],[11]

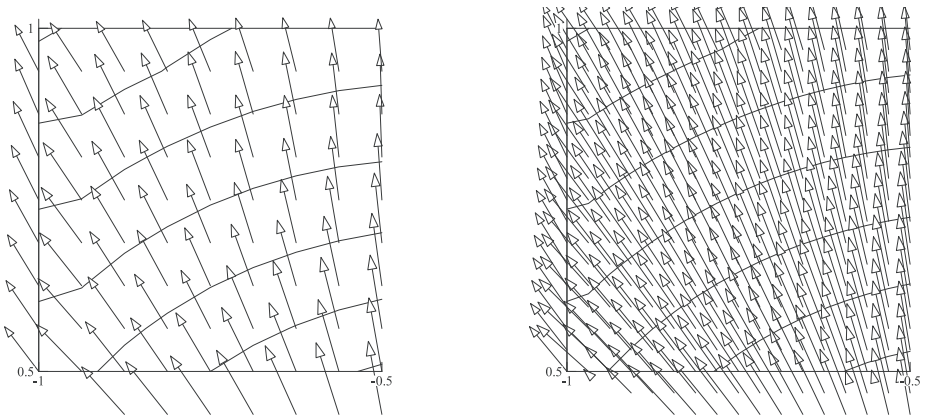

(a) Grid S1 (b) Grid S2

Figure 3 Level set contours and normal vectors of problem 3.1.

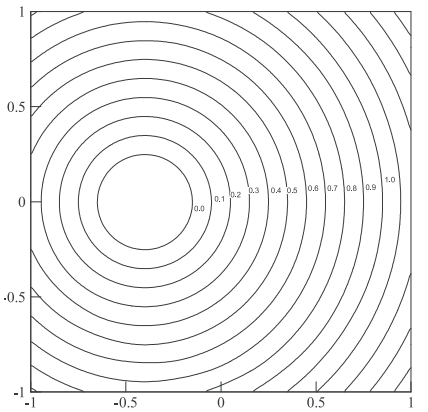

Figure 4 Level set contours of grid S4 at time *t=2* of problem 3.1.

$$\left\|L_{1,I}\right\| = \frac{1}{L}\int_{\Omega}\left|H(\phi_{numerical}) - H(\phi_{exact})\right|d\mathbf{x} \qquad (17)$$

where L is the perimeter size of interface. The Heaviside function H is given by $H(\phi)$ if $\phi < 0$ and $H(\phi) = 0$ otherwise. The $L_{1\,A}$-norm of the numerical error is also used to measure the area conservative property during evolution of an interface which is defined by

$$\left\|L_{1,A}\right\| = \left|\frac{A_T - A_0}{A_0}\right| \qquad (18)$$

where $A_n = \int_{\Omega} H(\phi^n)d\mathbf{x}$.

The values of error norms and rate of convergence are presented in Table 1. The table shows that the solution converges as the grid is refined with the convergence rate of about two.

Table 1 Errors and order of convergence of problem 3.1

Grid size	$\left\|L_{1\,I}\right\|$	$\left\|L_{1,A}\right\|$
S1	0.48215	0.02617
S2	0.11482	0.00324
S3	0.02583	0.00014
S4	0.00560	0.00010
Convergence order	**2.14**	**2.67**

3.2 Time-reversed Vortex Test

The third benchmark problem is a rotation of a circle with time-dependent flow field in a square domain of $\Omega = (0,0)\times(1,1)$. Initially, the circle with radius of 0.15 is centered at (0.5, 0.75) and is circulated with a time dependent velocity field given by [10],[12]

$$V(\boldsymbol{x},t) = (-\sin^2(\pi x)\sin(2\pi y)\cos(\pi t/T), \sin^2(\pi y)\sin(2\pi x)\cos(\pi t/T)) \qquad (19)$$

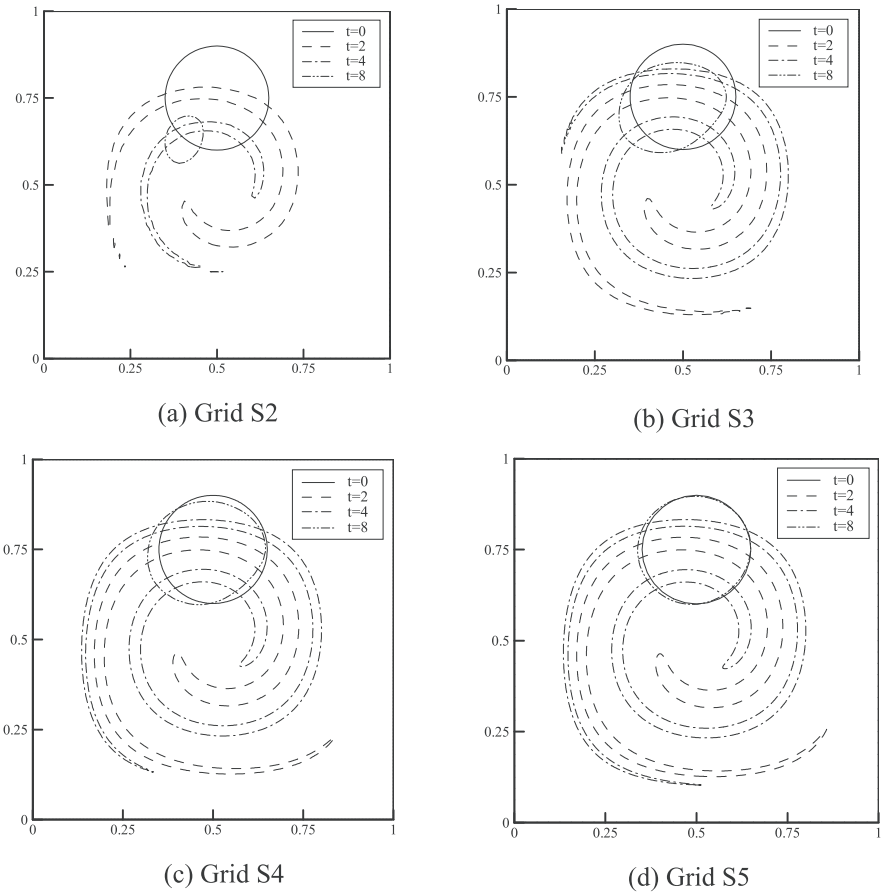

(a) Grid S2 (b) Grid S3

(c) Grid S4 (d) Grid S5

Figure 5 Comparison of numerical solutions of problem 3.2.

The given condition causes the flow to return to its initial state at time $t=T$ so that the quantitative error of the computed solution can be measured easily. The maximum distortion from initial interface shape occurs at $t=T/2$. As the reversal period T becomes longer, the interface stretches further away from its initial circular shape. To assess the performance and order of convergence of the scheme, the simulations are performed on the uniform square grids S2 to S5 consisting of 64×64 ($\Delta x=\Delta y=1/64$), 128×128, and 256×256, respectively. The problem is tested until the final time of where the flow field is reversed at time t=4. The zero level contour plots of the numerical solutions obtained from grids S2 to S5 at the times of 0, 2, 4 and 8 are shown in Figs. 5(a)-(d). From the results shown in these figures, there is no remarkable pinch off even by using the coarsen grid sizes. Figure 6 shows the area error resulted from using the S grid. For this example, the area error ε_M, is determined from

$$\varepsilon_M = \frac{A(t)-A_0}{A_0} \tag{20}$$

where A_0 is a area at time t=0.

The proposed method provides slight temporary mass loss on the finer grids. It is noted that the coarsen grids, such as grids S2 and S3, cannot provide

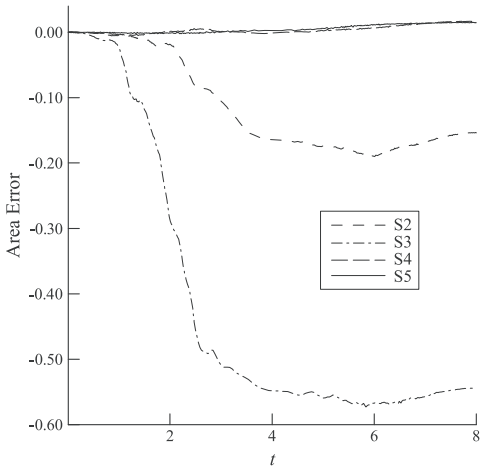

Figure 6 Area error of numerical solutions S2 to S5 of problem 3.2.

satisfactory results due to the complication of the time-dependent velocity field. The finer grids, such as grid S4, are needed to provide solutions with acceptable accuracy. The most accurate solution is achieved by using the triangular grid S5 as observed by the flat line around zero. Values of the error norms and rate of convergence are presented in Table 2. Figure 7(a) shows the comparison of level set contours of $\phi = 0, \pm h, \pm 2h, \pm 3h$ at $t = 4$ at obtained from the S grid (grid S5). The same comparisons at are shown in Fig. 7(b). These figures show that the signed distance function is preserved during the simulation. Results from these examples have also shown that the proposed method does not need the reinitialization in order to heal the distorted and stretched level set field.

Table 2 Errors and order of convergence of problem 3.2

Grid size	$\|L_{1,I}\|$	$\|L_{1,A}\|$
S2	0.07614	0.83689
S3	0.03035	0.15323
S4	0.01628	0.03781
S5	0.00471	0.01481
Convergence order	**1.34**	**1.94**

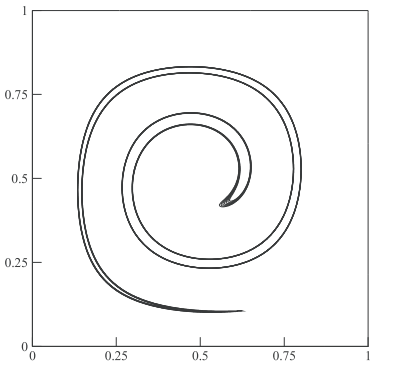

(a) $t = 4$

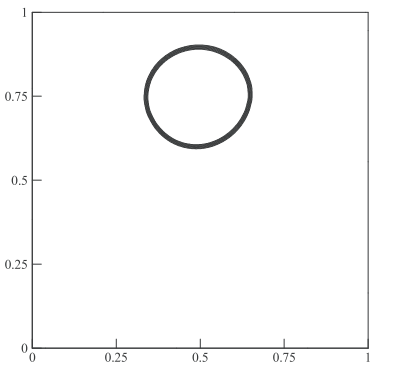

(b) $t = 8$

Figure 7 Level set contours of grid S5 of problem 3.2.

4. Conclusions

The paper presents an explicit finite volume method for solving the characteristic level set equation in two-dimensional domain. The theoretical formulation of the characteristic level set equation based on the characteristic-based scheme was explained. The finite volume method was applied to derive the discretized equations for the spatial domain. Four numerical examples were used to evaluate the performance and to determine the order of accuracy of the proposed method. These examples showed that the method provides second-order accurate and converged solution with improved accuracy as the grid is refined. Results from these examples have also shown that the proposed method does not need

the reinitialization in order to heal the distorted and stretched level set field.

5. Acknowledgements

The author is pleased to acknowledge King Mongkut's University of Technology North Bangkok, and the Office of the Higher Education Commission (OHEC), for supporting this research work.

References

[1] F.H. Harlow and J.E. Welch, "Numerical Calculation of Time-dependent Viscous Incompressible Flow of Fluid with Free Surface," *The Physics of Fluids*, vol. 8, pp. 2182-2189, 1965.

[2] C.W. Hirt and B.D. Nichols, "Volume of Fluid (VOF) Method for the Dynamics of Free Boundaries," *Journal of Computational Physics*, vol. 39, pp. 201-225, 1981.

[3] S. Osher and J.A. Sethian, "Fronts Propagating with Curvature-dependent Speed: Algorithms based on Hamilton-Jacobi Formulations," *J. Comput. Phys.* vol. 79, pp. 12-49, 1988.

[4] S. Osher and R. Fedkiw, *Level Set Methods and Dynamic Implicit Surfaces*, New York: Springer, 2003.

[5] J.A. Sethian, *Level Set Methods and Fast Marching Methods*, Cambridge: Cambridge University Press, 1999.

[6] M. Duflot, "A Study of the Representation of Cracks with Level Sets," *International Journal for Numerical Methods in Fluids*, vol. 70, pp. 1261-1302, 2007.

[7] J. Choi and G. Son, "Numerical Study of Droplet Motion in a Microchannel with Different Contact Angles," *Journal of Mechanical Science and Technology*, vol. 22, pp. 2590-2599, 2008.

[8] S. Phongthanapanich and P. Dechaumphai, "A Characteristic-based Finite Volume Element Method for Convection-Diffusion-Reaction Equation," *Transactions of the CSME*, vol. 32, pp. 549-560, 2008.

[9] S. Phongthanapanich, "An Explicit Finite Volume Element Method without an Explicit Artificial Diffusion Term for Convection-Diffusion Equation on Triangular Grids," *Thammasart International Journal of Science and Technology*, vol. 15, pp. 69-80, 2010.

[10] E. Olsson and G. Kreis, "A Conservative Level Set Method for Two-phase Flow," *Journal of Computational Physics*, vol. 210, pp. 225-246, 2005.

[11] M. Sussman and E. Fatemi, "An Efficient, Interface-preserving Level Set Redistancing Algorithm and Its Application to Interfacial Incompressible Fluid Flow," *SIAM Journal on Scientific Computing*, vol. 20, pp. 1165-1191, 1999.

[12] R.J. LeVeque, "High-resolution Conservative Algorithms for Advection in Incompressible Flow," *SIAM Journal on Numerical Analysis*, vol. 33, pp. 627–665, 1996.